THE JOURNAL OF PHYSICAL CHEMISTRY B

ARTICLE

pubs.acs.org/JPCB

Determining Force Field Parameters Using a Physically Based Equation of State

Thijs van Westen,[†] Thijs J. H. Vlugt,[†] and Joachim Gross*[,†,‡]

[†]Process and Energy Laboratory, Delft University of Technology, Leeghwaterstraat 44, 2628CA Delft, The Netherlands

[‡]Institut für Technische Thermodynamik und Thermische Verfahrenstechnik, University of Stuttgart, Pfaffenwaldring 9, 70569 Stuttgart, Germany

ABSTRACT: Force field parameters used in classical molecular simulations can be estimated from quantum mechanical calculations or spectroscopic measurements. This especially applies to bonded interactions such as bond-stretching, bond-bending, and torsional interactions. However, it is difficult and computational expensive to obtain accurate parameters describing the nonbonded van der Waals interactions from quantum mechanics. In many studies, these parameters are adjusted to reproduce experimental data, such as vapor−liquid equilibria (VLE) data. Adjusting these force field parameters to VLE data is currently a cumbersome and computationally expensive task. The reason is that the result of a calculation of the vapor−liquid equilibria depends on the van der Waals interactions of all atom types in the system, therefore requiring many time-consuming iterations. In this work, we use an analytical equation of state, the perturbed chain statistical associating fluid theory (PC-SAFT), to predict the results of molecular simulations for VLE. The analytical PC-SAFT equation of state is used to approximate the objective function $f(\mathbf{p})$ as a function of the array of force field parameters $\mathbf{p}$. The objective function is here for example defined as the deviations of vapor pressure, enthalpy of vaporization and liquid density data, with respect to experimental data. The parameters are optimized using the analytical PC-SAFT equation of state, which is orders of magnitude quicker to calculate than molecular simulation. The solution is an excellent approximation of the real objective function, so that the resulting method requires only very few molecular simulation runs to converge. The method is here illustrated by optimizing transferable Lennard-Jones parameters for the *n*-alkane series. Optimizing four force field parameters $\mathbf{p} = (\varepsilon_{CH_2CH_2}, \varepsilon_{CH_3CH_3}, \sigma_{CH_2CH_2}, \sigma_{CH_3CH_3})$ we obtain excellent agreement of coexisting densities, vapor pressure and caloric properties within only 2 −3 molecular simulation runs.

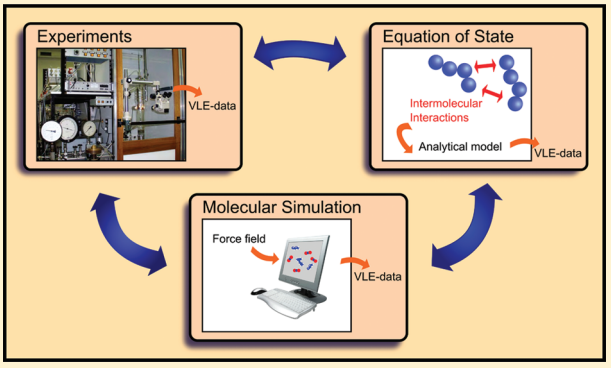

1. INTRODUCTION

One of the most prominent problems when applying molecular simulations to represent real substances is the choice of (or the optimization of) the force field parametrization.[1] With "parametrization" we here refer to both the choice of some functional form (such as Lennard-Jones or Buckingham potentials for van der Waals interactions), and the parameters of the considered functional form. Usually, interactions can be subdivided into bonded and nonbonded interactions. The parametrization that describes the bonded interactions is quite accurately obtained from quantum chemical calculations or spectroscopic data.[2−4] It is difficult and computationally expensive to obtain accurate parameters describing the nonbonded van der Waals interactions from quantum mechanics; in practice they are usually obtained by fitting molecular simulation results to experimental data. Vapor−liquid equilibrium (VLE) properties are particularly sensitive to the nonbonded interactions, so that force field parameters are often adjusted to accurately describe these data. It is well established that the van der Waals parametrization assigned to an atom in one molecule is fairly well transferable to the parametrization of the same atom in a different molecule.[3,5−8]

Different methods have been developed for fitting the nonbonded force field parameters to experimental data.[6−10] All of these are based on an iterative procedure. First, an initial guess of the force field parameters is used to perform a set of molecular simulations. Computed properties can be for example the vapor and liquid coexistence densities, vapor pressures and/or caloric properties such as enthalpy or energy of vaporization. An objective function is defined as the squared deviation between the experimental and the calculated values of these (or other) observables. Second, from these data, a next set of force field parameters is obtained, resulting in less deviations from the experimental data. This iterative process continues until the objective

Received: March 20, 2011
Revised: May 12, 2011
Published: May 13, 2011

function is minimal or lower than a certain specified value. Although the presently used fitting methods are based on this iterative procedure, different methods can be used for minimizing the objective function. Often, studies related to the optimization of force field parameters are somewhat unclear about the used method[3,5] which may suggest that no systematic minimization of a predefined objective function is used. Methods that perform well with respect to finding the minimum of an objective function are Simplex methods[11] or gradient based methods. The latter incorporate partial derivatives of the computed properties with respect to the force field parameters. Applications of the Simplex method are given in refs 6 and 9, for applications of gradient-based methods we refer the reader to refs 7, 8, and 10. Although the Simplex method is very robust in finding a local optimum, the convergence is slow, requiring many subsequent molecular simulation runs.[6,9,10] For gradient based methods, this number is lower, however, the time needed per simulation is larger since calculating partial derivatives of ensemble averages requires considerably longer simulations than just calculating ensemble averages.[1,8]

Clearly, a serious drawback of present fitting methods is that each iteration requires a time-consuming molecular simulation run. In this study, a method is developed that overcomes this limitation by performing the actual optimization of the nonbonded force field parameters in a different, faster, framework than molecular simulation, i.e., using the PC-SAFT equation of state (EOS).[12] PC-SAFT correlates the phase equilibrium properties for a large variety of molecules[12−14] with relatively high accuracy. Relating the PC-SAFT parameters to the nonbonded force field parameters enables us to predict the results of molecular simulations with good accuracy. Since PC-SAFT calculations are orders of magnitude faster than molecular simulations, the computational cost of our approach is significantly reduced compared to conventional optimization methods. The PC-SAFT EOS is based on a more coarse-grained molecular model compared to the force field based models used in molecular simulations. The molecular model, however, is rich enough to capture the size and nonspherical shape of molecules and the dispersive attraction of these fluids.[12−14] A physical basis of the analytic EOS is essential because it is then possible to directly relate the pure component parameters of the analytic EOS to the force field parameters.

This paper is organized as follows. In section 2, we show how the model parameters of PC-SAFT are related to force field parameters used in molecular simulations and we will show how this can be used to optimize force fields in an efficient way. In section 3, we describe the details of the molecular simulations used for obtaining VLE data. As a test case, the proposed method is used to obtain Lennard-Jones parameters accurately describing experimental VLE data of *n*-alkanes. This is shown in section 4. We show that only 2−3 iterations are needed. We summarize our findings in section 5.

2. THEORY

2.1. Force Field of *n*-Alkanes as a Test Case. We consider *n*-alkanes as simple molecules to illustrate the proposed approach. A united-atom approach is used in which a carbon atom and its adjacent hydrogen atoms are defined as a single interaction site. The Lennard-Jones (LJ) pair potential is used to describe the interactions between united atoms

$$u_{\alpha\beta}(r_{\alpha\beta}) = 4\varepsilon_{\alpha\beta}\left[\left(\frac{\sigma_{\alpha\beta}}{r_{\alpha\beta}}\right)^{12} - \left(\frac{\sigma_{\alpha\beta}}{r_{\alpha\beta}}\right)^{6}\right] \quad (1)$$

In this equation, $\sigma_{\alpha\beta}$ and $\varepsilon_{\alpha\beta}$ denote the LJ size- and energy parameter of two interacting sites, respectively. Further, $r_{\alpha\beta}$ denotes the distance between two interacting sites of type α and β. The interactions are only considered between pairs of sites α and β located on different molecules or for two sites within a molecule that are separated by more than three bonds.[3] For interactions between different atom types, the well-known Lorentz−Berthelot combining rules are used:[15]

$$\sigma_{\alpha\beta} = \frac{\sigma_{\alpha\alpha} + \sigma_{\beta\beta}}{2} \quad (2)$$

$$\varepsilon_{\alpha\beta} = \sqrt{(\varepsilon_{\alpha\alpha}\varepsilon_{\beta\beta})} \quad (3)$$

In the literature, many different united-atom LJ parameters for *n*-alkanes have been proposed.[3,5,16−20] In this work, we have chosen to use different σ and ε parameters for all interaction sites, i.e., $\sigma_{CH_2CH_2} \neq \sigma_{CH_3CH_3}$ and $\varepsilon_{CH_2CH_2} \neq \varepsilon_{CH_3CH_3}$, which is analogue to the popular TraPPE force field.[3] For a more historical perspective on the development of UA LJ parameters for *n*-alkanes, the reader is referred to ref 3.

The bonded interactions comprise bond-stretching (two consecutive atoms in a molecule), bond-bending (three consecutive atoms), and torsions (four consecutive atoms). Bond-stretching and bond-bending are both governed by a harmonic potential. For bond-stretching this potential is given by

$$u_{\text{stretch}} = K_b(b - b_0)^2/2 \quad (4)$$

where K_b/k_B = 96500 K Å^{-2} is the bond stretching constant (k_B being the Boltzmann constant), b is the bond length and b_0 = 1.54 Å is the equilibrium bond length[21] for both, CH_2-CH_2 bonds and CH_3-CH_2 bonds. The bond bending potential is given by

$$u_{\text{bend}} = K_\theta(\theta - \theta_0)^2/2 \quad (5)$$

with K_θ/k_B = 62500 K rad^{-2}, θ is the bond angle and θ_0 is the equilibrium bond angle which for *n*-alkanes is 114°.[21] The torsional rotations are described by the OPLS united-atom torsional potential

$$u_{\text{torsional}} = c_1[1 + \cos\phi] + c_2[1 - \cos 2\phi] + c_3[1 + \cos 3\phi] \quad (6)$$

with constants c_1/k_B = 355.03 K, c_2/k_B = − 68.19 K, and c_3/k_B = 791.32 K.[17]

2.2. Relating the PC-SAFT Equation of State to a Force Field Based Description of Molecules. To optimize the nonbonded force field parameters using the PC-SAFT EOS, we have to establish a relation between the force field parameters $\sigma_{\alpha\alpha}$ and $\varepsilon_{\alpha\alpha}$ and the PC-SAFT parameters. Figure 1 illustrates how both frameworks describe a "linear" chain molecule. PC-SAFT considers molecules as chains of freely jointed identical tangent sphere segments. Each segment is defined as an interaction site.[12] For nonassociating, nonpolar molecules such as *n*-alkanes, the chains are specified by the number of tangent spheres $\hat{m}$, an

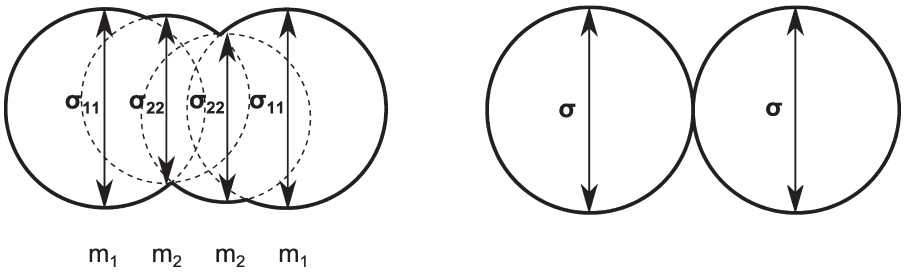

Figure 1. Schematic representation of a linear chain molecule using the force field based approach (left) and the PC-SAFT framework (right). PC-SAFT describes the molecule as a homonuclear chain of m freely jointed tangent sphere segments of size σ. Note that the value of m is not restricted to integers. In the force field based approach, a molecule is described as a heteronuclear chain of (partially) fused sphere segments. The chain configuration is governed by a bond bending potential. The size of a segment of type α is denoted by $\sigma_{\alpha\alpha}$. The parameter m_α, which is defined as the contribution of a fused sphere segment of type α to the effective PC-SAFT chain length m, is solely used to link both frameworks (eq 7).

effective segment size $\hat{\sigma}$ and an effective potential well depth $\hat{\varepsilon}$. Noninteger values for the segment number $\hat{m}$ are allowed. PC-SAFT requires no additional parameters for the intramolecular interactions, because these interactions are captured as averages by the ideal gas Helmholtz free energy term of the equation of state. The molecular model in the force field based approach used in molecular simulations is different. Here molecules are described as heterosegmented fused spheres with well-defined bond-angle and torsional potentials, see Figure 1. In order to allow a transition from the force field approach to the simpler PC-SAFT model, a dimensionless parameter m_α is introduced, which describes the contribution of a fused sphere segment of type α to the number of segments in PC-SAFT ($\hat{m}$). According to a group contribution concept, each (united) atom type is characterized by only one (transferable) parameter m_α. The two frameworks are then related by relating the parameter sets $\{m_\alpha, \sigma_{\alpha\alpha}, \varepsilon_{\alpha\alpha}\}$ to $\{\hat{m}, \hat{\sigma}, \hat{\varepsilon}\}$. We now proceed to propose three relations that allow us to express the PC-SAFT equation of state in terms of the force field parameters.

Using the definition of m_α, i.e. the contribution of a fused sphere segment of type α to the effective PC-SAFT chain length $\hat{m}$, we trivially have

$$\hat{m} = \sum_{\alpha}^{\substack{\text{segment}\\ \text{types}}} N_\alpha m_\alpha \tag{7}$$

where N_α is the number of α-type segments per molecule. The m_α parameters are available for a large number of groups and can be taken from a group contribution method.[22]

A similar connection can be made for the "volume" of the molecule. For PC-SAFT, the volume that a molecule occupies is approximated by the volume of $\hat{m}$ spheres of "diameter" $\hat{\sigma}$. For a force field based approach, again one has to account for the overlap between neighboring segments. As m_α describes the contribution of segment type α to the chain length, we can relate $\hat{\sigma}$ and $\sigma_{\alpha\alpha}$ by requiring that the volume of a molecule in PC-SAFT and in the force field based approach should be equal

$$\frac{\pi}{6}\hat{m}\hat{\sigma}^3 \approx \sum_{\alpha}^{\substack{\text{segment}\\ \text{types}}} \frac{\pi}{6} N_\alpha m_\alpha \sigma_{\alpha\alpha}^3 \tag{8}$$

A parameter ϕ_σ is introduced to correct for any approximation made in eq 8

$$\hat{m}(\hat{\sigma}\phi_\sigma)^3 = \sum_{\alpha}^{\substack{\text{segment}\\ \text{types}}} N_\alpha m_\alpha \sigma_{\alpha\alpha}^3 \tag{9}$$

We will show that in practice, the value of ϕ_σ is close to unity and it is not sensitive to temperature.

A relation between $\hat{\varepsilon}$ of the tangent sphere-chain (in PC-SAFT) and $\varepsilon_{\alpha\alpha}$ of the force field based approach can be derived based on perturbation theory. The dispersive attraction fluid is thereby treated as a perturbation to a repulsive reference fluid. A hard-chain fluid serves as the reference in the PC-SAFT equation of state. The Helmholtz energy F is then the sum of the ideal gas contribution, F^{ig}, the hard-chain reference term, F^{hc}, and attractive contributions,[12,23] as[12]

$$F = F^{ig} + F^{hc} + F^{disp} \tag{10}$$

Here, F^{disp} is the (attractive) dispersive contribution to the Helmholtz energy. We are not concerned with polar or associating molecules so that these contributions are here omitted. Lennard-Jones parameters were used in determining model constants of the PC-SAFT equation of state, so that an energy parameter, $\hat{\varepsilon}$, appears in the equation of state. For the purpose of relating the Lennard-Jones $\varepsilon_{\alpha\alpha}$-parameters (molecular simulation) to the $\hat{\varepsilon}$-parameter (PC-SAFT), we consider only the first-order perturbation term, which for a heterosegmented fluid reads

$$F^{disp} = 2\pi\rho N \sum_{\alpha}^{\substack{\text{segment}\\ \text{types}}} \sum_{\beta}^{\substack{\text{segment}\\ \text{types}}} N_\alpha N_\beta \int g_{\alpha\beta}(r) u_{\alpha\beta}^{disp}(r) r^2 \, dr \tag{11}$$

where, ρ is the number density of molecules in the system, N_α is the number of segments of type α in a molecule, $g_{\alpha\beta}(r)$ is the segment−segment radial distribution function and $u_{\alpha\beta}^{disp}(r)$ is the perturbing attractive part of the intermolecular potential. The double summation over all segment types is required to account for all segment−segment interactions of two interacting molecules. This first order perturbation term, eq 11, can be applied to both, a tangent hard-sphere model as well as a fused spheres model. That allows us to link the PC-SAFT model to the force field based approach. Denoting a hard-chain made up of tangent

hard spheres (PC-SAFT) by "hc" and a molecule made up of fused spheres (force field based approach) by 'fs' we equate the first order contributions of both frameworks, as

$$\sum_{\hat{\alpha}=1}^{\hat{m}}\sum_{\hat{\beta}=1}^{\hat{m}}\int \hat{g}^{\mathrm{hc}}_{\hat{\alpha}\hat{\beta}}(r)\hat{u}^{\mathrm{disp}}(r)r^2\,\mathrm{d}r = \sum_{\alpha}^{\substack{\text{segment}\\ \text{types}}}\sum_{\beta}^{\substack{\text{segment}\\ \text{types}}} N_\alpha N_\beta \int g^{\mathrm{fs}}_{\alpha\beta}(r)u^{\mathrm{disp}}_{\alpha\beta}(r)r^2\,\mathrm{d}r \qquad (12)$$

Note that for PC-SAFT (left-hand side of this equation) the intermolecular potential $u^{\mathrm{disp}}(r)$ has no segment type dependence because the PC-SAFT interaction parameters $\hat{\sigma}$ and $\hat{\varepsilon}$ are identical for all segment types. Because of this, the double summation on the lhs of this equations is not over segment types but over the number of PC-SAFT segments ($\hat{m}$). In addition, a mean hard-chain segment−segment radial distribution function $\bar{g}^{\mathrm{hc}}(r)$ is introduced, as defined by Chiew et al.[24]

$$\bar{g}^{\mathrm{hc}}(r) = \frac{1}{\hat{m}^2}\sum_{\hat{\alpha}=1}^{\hat{m}}\sum_{\hat{\beta}=1}^{\hat{m}}\hat{g}^{\mathrm{hc}}_{\hat{\alpha}\hat{\beta}}(r) \qquad (13)$$

The left-hand side of eq 12 then loses the double summation over PC-SAFT segments as

$$\hat{m}^2\int \bar{g}^{\mathrm{hc}}(r)\hat{u}^{\mathrm{disp}}(r)r^2\,\mathrm{d}r = \sum_{\alpha}^{\substack{\text{segment}\\ \text{types}}}\sum_{\beta}^{\substack{\text{segment}\\ \text{types}}} N_\alpha N_\beta \int g^{\mathrm{fs}}_{\alpha\beta}(r)u^{\mathrm{disp}}_{\alpha\beta}(r)r^2\,\mathrm{d}r \qquad (14)$$

For a force field that considers a LJ potential for the dispersive interactions, the equation above is made dimensionless by introducing a reduced radial distance $\tilde{r}$ and a reduced potential function $\tilde{u}^{\mathrm{disp}}$. For the left-hand side these are defined as $\tilde{r} = \mathrm{r}/\hat{\sigma}$ and $\tilde{u}^{\mathrm{disp}} = u^{\mathrm{disp}}(\tilde{r})/\hat{\varepsilon}$, for the right-hand side these are defined as $\tilde{r} = r/\sigma_{\alpha\beta}$ and $\tilde{u}^{\mathrm{disp}}(\tilde{r}) = u^{\mathrm{disp}}_{\alpha\beta}(\tilde{r})/\varepsilon_{\alpha\beta}$. By introducing these, the PC-SAFT parameters and the LJ parameters can be placed outside the integrals as

$$\hat{m}^2\hat{\sigma}^3\hat{\varepsilon}\int \bar{g}^{\mathrm{hc}}(\tilde{r})\tilde{u}^{\mathrm{disp}}(\tilde{r})\tilde{r}^2\,\mathrm{d}\tilde{r} = \sum_{\alpha}^{\substack{\text{segment}\\ \text{types}}}\sum_{\beta}^{\substack{\text{segment}\\ \text{types}}} N_\alpha N_\beta \sigma^3_{\alpha\beta}\varepsilon_{\alpha\beta}\int g^{\mathrm{fs}}_{\alpha\beta}(\tilde{r})\tilde{u}^{\mathrm{disp}}(\tilde{r})\tilde{r}^2\,\mathrm{d}\tilde{r} \qquad (15)$$

In order to derive a simple equation that relates force field parameters to PC-SAFT parameters, a critical assumption is made: the parameter-weighted average of the correlation integrals on the right-hand side of eq 15 is equal to the average correlation integral on the left-hand side of eq 15. This is supported by ref 25. Making this assumption, the integrals in eq 15 cancel, and we simply get

$$\hat{m}^2\hat{\sigma}^3\hat{\varepsilon} \approx \sum_{\alpha}^{\substack{\text{segment}\\ \text{types}}}\sum_{\beta}^{\substack{\text{segment}\\ \text{types}}} N_\alpha N_\beta \sigma_{\alpha\beta}{}^3\varepsilon_{\alpha\beta} \qquad (16)$$

To correct for the assumptions made for deriving this equation, a second correction parameter ϕ_ε is introduced, as

$$\hat{m}^2(\hat{\sigma}\phi_\sigma)^3(\hat{\varepsilon}\phi_\varepsilon) = \sum_{\alpha}^{\substack{\text{segment}\\ \text{types}}}\sum_{\beta}^{\substack{\text{segment}\\ \text{types}}} N_\alpha N_\beta \sigma_{\alpha\beta}{}^3\varepsilon_{\alpha\beta} \qquad (17)$$

where, for consistency with eq 9, we include the ϕ_σ correction parameter as well. Like the ϕ_σ parameter, the ϕ_ε parameter is in practice close to unity and it is not sensitive to the temperature. The three relations, eq 7, eq 9, and eq 17, can be written explicitly in $\{m, \hat{\sigma}, \text{and } \hat{\varepsilon}\}$ so that the PC-SAFT equation of state is expressed explicitly in terms of the force field parameters.

Equation 16 was derived for force fields that use a 12-6 LJ potential to describe the interactions of nonassociating molecules. Using a LJ *n-m* potential different than the 12-6 potential would only introduce a weakly temperature dependent factor on one side of eq 16. This factor can approximately be absorbed by the constant correction parameter ϕ_ε. This makes eq 17 applicable to force fields other than the LJ 12-6 potential, such as the Mie potential or the Buckingham potential.

2.3. Procedure for Parameter Optimization. The objective is now to optimize the nonbonded force field parameters $\sigma_{\alpha\alpha}$ and $\varepsilon_{\alpha\alpha}$ to experimental pure component VLE data. Our procedure uses the PC-SAFT EOS for estimating the outcome of molecular simulations. The general principle is, that we define an objective function $f(\mathbf{p})$ with $\mathbf{p}$ as the array of adjustable force field parameters (here, $\mathbf{p} = (\varepsilon_{\mathrm{CH_3CH_2}}, \varepsilon_{\mathrm{CH_3CH_3}}, \sigma_{\mathrm{CH_2CH_2}}, \sigma_{\mathrm{CH_3CH_3}})$). Using an initial guess for the force field parameters ($\mathbf{p}^0$), molecular simulations are conducted to obtain a value of the objective function. Next, the PC-SAFT equation of state is used, with eq 7, eq 9, eq 17, to (approximately) minimize the objective function. The resulting parameter vector $\mathbf{p}^1$ is subsequently used in molecular simulation runs in order to evaluate the objective function. The procedure is repeated until a convergence criterion is satisfied. In case one would like to fit force field parameters ($\varepsilon_{\alpha\alpha}$, $\sigma_{\alpha\alpha}$) for more than one (united) atom simultaneously, it is de facto necessary to perform the procedure using experimental data for more than one molecule type. The reason is that in practice $\varepsilon_{\alpha\alpha}$ of one (united) atom α and $\varepsilon_{\beta\beta}$ of a second atom β within the same molecule are highly correlated. The same is true for the $\sigma_{\alpha\alpha}$ and $\sigma_{\beta\beta}$ parameters within one molecule. This observation is not specific to our procedure, but is generally observed. The proposed procedure for adjusting force field parameters is in more detail:

1. Choose an initial guess $\mathbf{p}^0$ of the force field parameters and take the m_α parameters from a PC-SAFT group contribution method.[22] For the remainder, m_α will be fixed.
2. For all molecule types, use the initial guess of the force field parameters to perform molecular simulations and compute the phase equilibrium properties of interest. These properties are denoted by Ω^{sim}, where Ω can for example represent vapor pressure data, liquid density data, and enthalpy of vaporization data. Calculate the objective function $f(\mathbf{p})$, as

$$f(\mathbf{p}) = \frac{1}{N^{\mathrm{exp}}}\sum_{n=1}^{N^{\mathrm{exp}}}\left(\frac{\Omega_n^{\mathrm{sim}}(\mathbf{p}) - \Omega_n^{\mathrm{exp}}}{\Omega_n^{\mathrm{exp}}}\right)^2 \qquad (18)$$

Here, N^{exp} is the number of experimental data points and Ω_n^{exp} represents the n^{th} experimental data point. If $f(\mathbf{p})$ or

dx.doi.org/10.1021/jp2026219 |J. Phys. Chem. B 2011, 115, 7872–7880

the gradient of f is lower than some specified tolerance, we accept the force field parameters as final values; if not, proceed with the next step.

3. Adjust the ϕ_σ and ϕ_ε parameters of eq 9 and eq 17 for each molecule type so that PC-SAFT EOS reproduces the molecular simulation data.
4. Use these correction parameters with eq 7, eq 9, and eq 17. The PC-SAFT EOS is henceforth explicitly expressed in terms of the force field parameters $\mathbf{p}$ and some selected observable Ω^{SAFT} can be calculated. The resulting value $\Omega^{\mathrm{SAFT}}(\mathbf{p})$ is an estimate of how PC-SAFT models the outcome of molecular simulations, explicitly in terms of the force field parameters $\mathbf{p}$. Now optimize these force field parameters to experimental data, in our case using a Levenberg−Marquardt algorithm[11] by minimizing the auxiliary objective function $f_{\mathrm{aux}}(\mathbf{p})$, with

$$f_{\mathrm{aux}}(\mathbf{p}) = \frac{1}{N^{\mathrm{exp}}} \sum_{n=1}^{N^{\mathrm{exp}}} \left(\frac{\Omega_n^{\mathrm{SAFT}}(\mathbf{p}) - \Omega_n^{\mathrm{exp}}}{\Omega_n^{\mathrm{exp}}} \right)^2 \qquad (19)$$

This auxiliary objective function only involves values Ω^{SAFT} calculated from the PC-SAFT equation of state so that the optimization is computationally very cheap.

5. Return to step 2 and use the new best guess of the force field parameters to repeat the cycle.

As the PC-SAFT EOS correctly describes the experimental VLE data, the fit using PC-SAFT is expected to be excellent and the objective function $f_{\mathrm{aux}}(\mathbf{p})$ will converge to a minimum value.

3. SIMULATION DETAILS

The Gibbs ensemble Monte Carlo (GEMC) method proposed by Panagiotopoulos[26,27] combined with Configurational-bias (re)growth moves[1,28,29] are used for computing VLE data for *n*-alkanes. The different Monte Carlo moves used in the simulations are volume exchange, particle transfer, translation, rotation and reinsertion. The relative probability of selecting a move is 0.0244 for volume exchange and 0.244 for all other moves. The maximum displacements for translation and rotation are adjusted such that on average 50% of these moves is accepted. Simulations are performed for systems of 300 molecules for butane and 200 molecules for hexane and octane. The total volume is chosen in such a way that after equilibration the vapor box is approximately of the same size as the liquid box. The Lennard-Jones potential was truncated at 14 Å and standard tail corrections[1] were applied. The number of Monte Carlo steps used for equilibration was at least 2.5 million and for production runs we used between 20 and 100 million Monte Carlo steps. The error in the estimate of the computed ensemble averages are calculated by dividing the production run into five blocks.

4. RESULTS AND DISCUSSION

The $m_{\mathrm{CH_3}}$ and $m_{\mathrm{CH_2}}$ parameters were obtained by fitting eq 7 to data for m for the C_2-C_{10} *n*-alkane series, taken from ref 12. Equation 7 describes this homologous series well, and the values for $m_{\mathrm{CH_3}} = 0.8083$ and $m_{\mathrm{CH_2}} = 0.3604$ are here used for butane, hexane, and octane. All experimental data used in this section is taken from ref.[30]

4.1. The Optimization of the CH_2 LJ Parameters. To test the proposed fitting procedure of section 2.3, we first consider the case in which the CH_2 LJ parameters of butane are optimized, while keeping the LJ parameters for CH_3 fixed. We define two observables, i.e., the liquid and the vapor density at $T = 295$ K, while the two LJ parameters for CH_2 are the degrees of freedom. The value of the objective function has to reduce to the level of the standard deviations of the molecular simulations in this case. The parameters of the CH_3 group are unchanged in this calculation and the values are taken from the TraPPE force field.[3]

Table 1. Results of Our Method for Determining the Optimal Lennard-Jones Parameters for CH_2 Using Experimental VLE Data for *n*-Butane at $T = 295$ K[a]

				AD (%)		
iteration no.	force field parameters	ϕ_σ	ϕ_ε	ρ_L	ρ_V	AAD (%)
initial guess	$\sigma_{\mathrm{CH_2}} = 3.95$ Å	1.0387	0.9653	0.01	41.54	$20.78_{1.54}$
	$\varepsilon_{\mathrm{CH_2}}/k_B = 46.0$ K					
1	$\sigma_{\mathrm{CH_2}} = 4.04$ Å	1.0400	0.9577	0.79	5.85	$3.32_{1.66}$
	$\varepsilon_{\mathrm{CH_2}}/k_B = 49.4$ K					
2	$\sigma_{\mathrm{CH_2}} = 4.05$ Å	1.0401	0.9554	0.12	1.47	$0.80_{1.14}$
	$\varepsilon_{\mathrm{CH_2}}/k_B = 48.4$ K					
3	$\sigma_{\mathrm{CH_2}} = 4.05$ Å			0.07	1.06	$0.38_{1.11}$
	$\varepsilon_{\mathrm{CH_2}}/k_B = 48.1$ K					

[a] The LJ parameters for CH_3 are fixed and taken from the TraPPE force field. For each iteration step, the absolute relative deviation (AD) and average absolute relative deviation (AAD) of simulated properties to experimental data is presented. The subscript next to the AAD gives the standard deviation.

Table 1 shows the optimization of the $\sigma_{\mathrm{CH_2}}$ and $\varepsilon_{\mathrm{CH_2}}$ LJ force field parameters to experimental coexistence densities of butane. We used the TraPPE parameters as an initial guess. For each iteration, the absolute average deviation (AAD) of the predicted coexistence densities is presented together with its standard deviation. It is clear that using the standard TraPPE force field parameters for the CH_2 group, the liquid density is well reproduced but the density of the vapor significantly deviates from the experimental value. In only three iterations, both the liquid- and vapor coexistence densities are very close to the experimental values. The statistical accuracy of our GEMC simulations is 0.1% for the liquid density and 2.3% for the vapor density. These results suggest that the PC-SAFT equation of state can be used to extrapolate the behavior of molecular simulations with good accuracy. The quick convergence of the procedure indicates that the objective function $f_{\mathrm{aux}}(\mathbf{p})$ is a good approximation for the true objective function $f(\mathbf{p})$. The observation that one iteration is not sufficient can be attributed to the fact that the correction parameters $\phi\sigma$ and $\phi\varepsilon$ are not entirely constant throughout the optimization (see Table 1).

To test the method for robustness we also performed the optimization for an initial guess of the $\sigma_{\mathrm{CH_2}}$ and $\varepsilon_{\mathrm{CH_2}}$ LJ force field parameters that is far away from the TraPPE parameters. We used $\sigma_{\mathrm{CH_2}} = 2.50$ Å and $\varepsilon_{\mathrm{CH_2}}/k_B = 90.0$ *K* as an initial guess while the TraPPE parameters are $\sigma_{\mathrm{CH_2}} = 3.95$ Å and $\varepsilon_{\mathrm{CH_2}}/k_B = 46.0$ *K*. We show the course of this optimization in Table 2. Both the optimized force field parameters and the correction parameters are included. The results clearly show that within only three iterations, the force field parameters are very close to the optimal parameters from Table 1. Clearly, the method is perfectly able to converge when using a "bad" initial guess of the force field parameters.

4.2. The Simultaneous Optimization of the CH_2 and CH_3 Parameters. The results for the simultaneous optimization of the CH_2 and CH_3 Lennard-Jones force field parameters are presented in Table 3 and Table 4. Table 3 shows the *n*-butane/*n*-hexane system and Table 4 shows the results for the *n*-butane/*n*-octane system. The optimal results are marked by an asterisk. This case represents a parameter optimization problem, where the number of degrees of freedom (4) is lower than the number experimental data points. It is therefore expected that the objective function does not converge to zero as a minimal value.

The TraPPE force field parameters serve as an initial guess for these calculations.The results in Table 3 confirm that for the original TraPPE parametrization, the liquid densities are in excellent agreement with the experimental data, whereas the deviations in vapor density/pressure are in the range of 30%. In the course of two to three iterations, the procedure converges to a low value of the objective function. The results for the vapor densities and internal energies of vaporization are significantly improved with respect to TraPPE. Although we did not include vapor pressures in the objective function, we have added

Table 2. Optimized Force Field Parameters and Correction Parameters for the Same Optimization As Presented in Table *1* Using a Different Initial Guess of the σ_{CH_2} and ε_{CH_2} LJ Force Field Parameters

iteration no.	force field parameters	ϕ_σ	ϕ_ε
initial guess	σ_{CH_2} = 2.50 Å	1.0110	1.1757
	ε_{CH_2}/k_B = 90.0 K		
1	σ_{CH_2} = 3.72 Å	1.0375	0.9982
	ε_{CH_2}/k_B = 81.7 K		
2	σ_{CH_2} = 4.02 Å	1.0400	0.9587
	ε_{CH_2}/k_B = 53.4 K		
3	σ_{CH_2} = 4.05 Å	1.0406	0.9560
	ε_{CH_2}/k_B = 48.6 K		

Table 3. Results of Our Method for Determining the Optimal Lennard-Jones Parameters for CH_2 and CH_3 Using Experimental VLE Data for *n*-Butane and *n*-Hexane[a]

					AD (%)					
iteration no.	force field parameters	component	ϕ_σ	ϕ_ε	T/[K]	p^{vap}	ρ_L	ρ_V	$\Delta^{LV}u$	AAD (%)
initial guess	σ_{CH_3} = 3.75 Å	*n*-butane	1.0390	0.9637	295	42.97	0.04	44.12	8.63	
	ε_{CH_3}/k_B = 98.0 K				327	33.43	0.05	34.92	8.15	
	σ_{CH_2} = 3.95 Å				360	31.63	0.45	29.60	8.83	
	ε_{CH_2}/k_B = 46.0 K	*n*-hexane	1.0220	1.0426	350	38.60	0.39	38.67	7.60	
					387	34.99	0.42	35.81	6.54	
					432	23.60	0.49	23.68	7.08	
						AAD (%)	0.30	34.47	7.81	$14.19_{1.29}$
1	σ_{CH_3} = 3.79 Å	*n*-butane	1.0388	0.9560	295	3.25	0.51	4.61	1.98	
	ε_{CH_3}/k_B = 103 K				327	3.89	1.12	6.49	0.16	
	σ_{CH_2} = 3.97 Å				360	5.80	2.19	9.89	1.87	
	ε_{CH_2}/k_B = 46.8 K	*n*-hexane	1.0228	1.0329	350	2.72	0.99	3.94	1.32	
					387	5.81	1.27	8.46	0.89	
					432	6.77	2.21	11.99	3.50	
						AAD (%)	1.38	7.56	1.62	$3.52_{0.67}$
2*	σ_{CH_3} = 3.78 Å	*n*-butane	1.0396	0.9559	295	3.16	0.05	2.16	2.99	
	ε_{CH_3}/k_B = 102 K				327	0.38	0.25	2.59	1.72	
	σ_{CH_2} = 3.99 Å				360	2.20	1.95	0.28	0.26	
	ε_{CH_2}/k_B = 46.1 K	*n*-hexane	1.0234	1.0318	350	1.88	0.22	0.78	2.96	
					387	3.58	0.74	1.84	0.58	
					432	1.11	0.97	5.35	0.89	
						AAD (%)	0.7	2.17	1.57	$1.48_{0.92}$
3	σ_{CH_3} = 3.79 Å	*n*-butane	1.0373	0.9559	295	2.68	0.22	0.24	3.19	
	ε_{CH_3}/k_B = 103 K				327	1.33	0.22	3.29	1.55	
	σ_{CH_2} = 3.99 Å				360	4.24	1.21	7.81	0.34	
	ε_{CH_2}/k_B = 46.0 K	*n*-hexane	1.0233	1.0320	350	8.42	0.35	7.41	2.79	
					387	0.81	0.19	3.01	0.96	
					432	0.26	0.83	4.17	0.68	
						AAD (%)	0.5	4.32	1.59	$2.14_{0.69}$

[a] The procedure is started using the parameters from the TraPPE force field. Here, the coexistence densities as well as the internal energy of evaporation are used to fit the force field parameters. Results for the vapour pressure are included as well. For each iteration step, the absolute relative deviation (AD) and average absolute relative deviation (AAD) of simulated properties to experimental data is presented. The subscript next to the AAD gives the standard deviation. The asterisk indicates the optimal result.

dx.doi.org/10.1021/jp2026219 |*J. Phys. Chem. B* 2011, 115, 7872–7880

Table 4. Results of Our Method for Determining the Optimal Lennard-Jones Parameters for CH_2 and CH_3 Using Experimental VLE Data for *n*-Butane and *n*-Octane[a]

					AD (%)				
iteration no.	force field parameters	component	ϕ_σ	ϕ_ε	T/[K]	ρ_L	ρ_V	$\Delta^{LV}u$	AAD (%)
initial guess	σ_{CH_3} = 3.75 Å	*n*-butane			295	0.04	44.12	9.66	
	ε_{CH_3}/k_B = 98.0 K		1.0390	0.9637	327	0.05	34.92	9.26	
	σ_{CH_2} = 3.95 Å				360	0.45	29.60	10.19	
	ε_{CH_2}/k_B = 46.0 K	*n*-octane			392	0.54	29.51	8.35	
			1.0104	1.0943	440	0.27	34.00	7.48	
					488	0.47	20.89	7.96	
					AAD (%)	0.30	32.18	8.82	$13.77_{1.24}$
1	σ_{CH_3} = 3.80 Å	*n*-butane	1.0402	0.9577	295	0.57	3.05	2.13	
	ε_{CH_3}/k_B = 103 K				327	1.08	5.12	0.23	
	σ_{CH_2} = 3.96 Å				360	2.45	7.25	2.11	
	ε_{CH_2}/k_B = 46.6 K	*n*-octane	1.0137	1.0898	392	1.22	0.42	2.33	
					440	2.03	0.68	0.59	
					488	2.07	9.91	2.07	
					AAD (%)	1.57	4.4	1.57	$2.52_{0.69}$
2	σ_{CH_3} = 3.79 Å	*n*-butane	1.0378	0.9519	295	0.24	5.00	3.14	
	ε_{CH_3}/k_B = 102 K				327	0.47	2.97	1.15	
	σ_{CH_2} = 3.98 Å				360	1.09	10.24	0.79	
	ε_{CH_2}/k_B = 46.5 K	*n*-octane	1.0138	1.0833	392	0.91	6.00	2.46	
					440	1.26	6.24	0.80	
					488	1.59	14.56	3.01	
					AAD (%)	0.92	7.5	1.89	$3.44_{0.78}$
3*	σ_{CH_3} = 3.77 Å	*n*-butane	1.0382	0.9551	295	0.02	6.62	4.18	
	ε_{CH_3}/k_B = 101 K				327	0.03	0.20	3.06	
	σ_{CH_2} = 4.00 Å				360	1.44	0.86	0.96	
	ε_{CH_2}/k_B = 46.1 K	*n*-octane	1.0134	1.0783	392	0.19	6.97	3.67	
					440	1.02	1.40	0.50	
					488	1.13	8.02	0.91	
					AAD (%)	0.64	4.01	2.21	$2.29_{1.00}$
4	σ_{CH_3} = 3.78 Å	*n*-butane			295	0.03	3.09	3.90	
	ε_{CH_3}/k_B = 103 K				327	0.53	1.25	2.30	
	σ_{CH_2} = 3.99 Å				360	1.21	3.68	0.40	
	ε_{CH_2}/k_B = 45.5 K	*n*-octane			392	0.51	14.42	3.83	
					440	0.40	5.71	2.84	
					488	0.71	1.07	0.35	
					AAD (%)	0.56	4.87	2.27	$2.57_{0.75}$

[a] The procedure is started using the parameters from the TraPPE force field. Here, the coexistence densities as well as the internal energy of evaporation are used to fit the force field parameters. For each iteration step, the absolute relative deviation (AD) and average absolute relative deviation (AAD) of simulated properties to experimental data is presented. The subscript next to the AAD gives the standard deviation. The asterisk indicates the optimal result.

computed vapor pressures in Table 3 to show the equivalence between the vapor density and pressure. Clearly the optimization of the vapor densities indirectly leads to optimized vapor pressures as well. The deviations in the liquid densities are slightly increased compared to the TraPPE force field, because now the force field parameters are also fitted to reproduce the vapor density and the internal energy of vaporization. For the *n*-butane/*n*-octane system we estimated the critical temperature T_C and density ρ_C from linear fits of the subcritical simulation data to respectively the density scaling law,[1]

$$\rho_L - \rho_V = B(T - T_C)^\beta \tag{20}$$

and the law of rectilinear diameters[1]

$$\frac{1}{2}(\rho_L + \rho_V) = \rho_C + A(T - T_C) \tag{21}$$

dx.doi.org/10.1021/jp2026219 |J. Phys. Chem. B 2011, 115, 7872–7880

Table 5. Predicted Critical Properties from our Force Field (Obtained from the *n*-Butane/*n*-Octane Fit, As Presented in Table 4) and TraPPE Compared to Experimental Values[a]

				AD (%)	
alkane	force field	T_C/K	ρ_C/kg m^{-3}	T_C	ρ_C
butane	present work	435	231	2.3	1.4
	TraPPE	423	231	0.5	1.4
	experimental	425.18	227.9		
octane	present work	586	231	3.2	0.5
	TraPPE	568	240	0.1	3.4
	experimental	568.841	232.2		

[a] Absolute average deviations (AD) of the estimated critical properties from experimental values are presented as well.

Here, A and B are constants and the critical exponent β is taken to be 0.32. The absolute average deviations of the estimated critical properties from experimental data are presented in Table 5 and compared to the deviations for TraPPE. Although our force field predicts somewhat better critical densities, critical temperatures are overpredicted to about 3%. This is less accurate than TraPPE, which overpredicts critical temperatures to about 0.5%. Clearly, the penalty for better predicting the vapor densities/pressure is a slightly worse prediction of the critical temperature. This result indicates limitations in the use of a UA methodology in combination with a LJ 12-6 potential for describing the phase behavior of *n*-alkanes.

To evaluate the effect of statistical noise generated by the uncertainties in the molecular simulations, it was attempted to further optimize the optimal force field parameters for the butane/hexane system using three times as long production runs for the GEMC simulations. Although this reduced the statistical uncertainty in the AAD to approximately 0.3%, the outcome of this optimization showed no further improvements in the obtained AAD. This also suggests that the use of a Lennard-Jones potential together with a UA methodology is limiting here.

The optimal force field parameters, obtained by fitting to the *n*-butane/*n*-hexane and *n*-butane/*n*-octane systems respectively, are nearly identical suggesting that these parameters may be considered as an improvement of the TraPPE force field. However, more systematic tests using a larger experimental data set are required to draw conclusions on this point.

5. CONCLUSIONS

The procedure presented in this work uses a physically based equation of state for optimizing nonbonded force field parameters. By formulating the analytical PC-SAFT EOS as a function of the force field parameters, it is possible to approximate the objective function for adjusting force field parameters within the PC-SAFT framework. This approach allows a gradient-based optimization of force field parameters using the equation of state without the need to perform a large number of computationally expensive molecular simulations.

The procedure was successfully illustrated for the optimization of the CH_2 12-6 LJ force field parameters of butane. Within only two molecular simulation runs, the experimental vapor and liquid coexistence densities at T = 295 K were reproduced with errors smaller than the statistical accuracy of the GEMC simulations. An initial guess of the force field parameters that is far away from the optimum only results in one extra iteration. Clearly, this optimization did not result in a set of transferable force field parameters, however, these results prove the principle of the proposed optimization procedure for force field parameters.

Next to this, the fitting procedure was used for the simultaneous optimization of the four Lennard-Jones parameters of CH_2 and CH_3 groups to pure component VLE data of *n*-butane/*n*-hexane and *n*-butane/*n*-octane. Different temperatures per molecule type were incorporated in the fit. Compared to predictions based on the well-known TraPPE force field for *n*-alkanes, all results showed great improvement of predicted vapor densities and internal energies of vaporisation. Liquid densities were predicted slightly worse. The observation that not all properties could be fitted to within the statistical accuracy of the GEMC simulations highlights limitations in the use of 12-6 LJ potential in combination with a united atom methodology for describing the VLE of *n*-alkanes. Recently, Potoff et al.[31] showed that the VLE data of the *n*-alkane series is much better described using a 16-6 LJ potential than the conventional 12-6 LJ potential. As our approach does not make significant assumptions concerning the power of the repulsive part of the potential, our method could be used to obtain the optimal function form of the n-m LJ potential as well as the optimal size- and energy parameter.

For future force field development, the results of the simultaneous optimization of the CH_2 and CH_3 force field parameters are promising. The present can be considered as a presentation of the concept together with a proof of principle. A goal for future work is to extend the method to other molecule types such as polar molecules and to decrease the statistical uncertainty of the simulation results by more advanced simulation techniques.[32,33]

AUTHOR INFORMATION

Corresponding Author

*E-mail: gross@itt.uni-stuttgart.de.

REFERENCES

(1) Frenkel, D.; Smit, B. *Understanding Molecular Simulation: from Algorithms to Applications*, 2nd ed.; Academic Press: San Diego, CA, 2002.

(2) Allinger, N. L.; Yuh, Y. H.; Lii, J. M. *J. Am. Chem. Soc.* **1989**, *111*, 8551–8566.

(3) Martin, M. J.; Siepmann, J. I. *J. Phys. Chem. B* **1998**, *102*, 2569–2577.

(4) Dubbeldam, D.; Calero, S.; Vlugt, T. J. H.; Krishna, R.; Maesen, T. L. M.; Smit, B. *J. Phys. Chem. B* **2004**, *108*, 12307–12313.

(5) Nath, S. K.; Escobedo, F. A.; de Pablo, J. J. *J. Chem. Phys.* **1998**, *108*, 9905–9911.

(6) Faller, R.; Schmitz, H.; Biermann, O.; Müller-Plathe, F. *J. Comput. Chem.* **1999**, *20*, 1009–1017.

(7) Ungerer, P.; Beauvais, C.; Delhommelle, J.; Boutin, A.; rousseau, B.; Fuchs, A. *J. Chem. Phys.* **2000**, *112*, 5499–5510.

(8) Bourasseau, E.; Haboudou, M.; Boutin, A.; Fuchs, A. H.; Ungerer, P. *J. Chem. Phys.* **2003**, *118*, 3020–3034.

(9) García-Sánchez, A.; Ania, C. O.; Parra, J. B.; Dubbeldam, D.; Vlugt, T. J. H.; Krishna, R.; Calero, S. *J. Phys. Chem. C* **2009**, *113*, 8814–8820.

(10) Hülsmann, M.; Köddermann, T.; Vrabec, J.; Reith, D. *Comput. Phys. Commun.* **2010**, *181*, 499–513.

(11) Press, W. H.; Teukolsky, S. H.; Vetterling, W. T.; Flannery, B. P. *Numberical Recipes in Fortran 77*; Cambridge University Press: Cambridge, U.K., 1992.

(12) Gross, J.; Sadowski, G. *Ind. Eng. Chem. Res.* **2001**, *40*, 1244–1260.

(13) Gross, J.; Sadowski, G. *Ind. Eng. Chem. Res.* **2002**, *41*, 5510–5515.
(14) Tumakaka, F.; Gross, J.; Sadowski, G. *Fluid Phase Equilib.* **2005**, *228*−*229*, 89–98.
(15) Allen, M. P.; Tildesley, D. J. *Computer simulation of liquids*; Oxford University Press: Oxford, U.K., 1987.
(16) Ryckaert, J. P.; Bellemans, A. *Chem. Phys. Lett.* **1975**, *30*, 123–125.
(17) Jorgensen, W. L.; Madura, J. D.; Swenson, C. J. *J. Am. Chem. Soc.* **1984**, *106*, 813.
(18) Siepmann, J. I.; Karaborni, S.; Smit, B. *Nature* **1993**, *365*, 330–332.
(19) Smit, B.; Karaborni, S.; Siepmann, J. I. *J. Chem. Phys.* **1995**, *102*, 2126–2140.
(20) Smit, B.; Karaborni, S.; Siepmann, J. *J. Chem. Phys.* **1998**, *109*, 352.
(21) van der Ploeg, P.; Berendsen, H. J. C. *J. Chem. Phys.* **1982**, *94*, 3271.
(22) Tihic, A.; Kontogeorgis, M.; von Solms, N.; Michelsen, M. L. *Ind. Eng. Chem. Res.* **2008**, *47*, 5092–5101.
(23) Gross, J.; Sadowski, G. *Fluid Phase Equilib.* **2000**, *168*, 183–199.
(24) Chiew, Y. C. *Mol. Phys.* **1991**, *73*, 359–373.
(25) Abu-Sharkh, B. F.; Sunaidi, A.; Hamad, E. Z. *J. Chem. Phys.* **2004**, *120*, 5795–5801.
(26) Panagiotopoulos, A. Z. *Mol. Phys.* **1987**, *61*, 813–826.
(27) Panagiotopoulos, A. Z. *Mol. Phys.* **1987**, *62*, 701–719.
(28) Siepmann, J. I.; Frenkel, D. *Mol. Phys.* **1992**, *75*, 59–70.
(29) Frenkel, D.; Mooij, G. C. A. M.; Smit, B. *J. Phys.: Condens. Matter* **1991**, *3*, 3053–3076.
(30) Smith, B. D.; Srivastava, R. *Thermodynamic data for pure compounds: Part A Hydrocarbons and ketones*; Elsevier: Amsterdam, 1986.
(31) Potoff, J. J.; Bernard-Brunel, A. *J. Phys. Chem. B* **2009**, *113*, 14725–14731.
(32) Binder, K. *Mol. Phys.* **2010**, *4* (108), 1797–1815.
(33) Virnau, P.; Möller, M. *J. Chem. Phys.* **2004**, *120*, 10925–10930.